5284 *Biochemistry* **2009,** *48,* 5284–5290
DOI: 10.1021/bi8020668

BIOCHEMISTRY
including biophysical chemistry & molecular biology
Article

Structure of the Cytoplasmic Loop between Putative Helices II and III of the Mannitol Permease of *Escherichia coli*: A Tryptophan and 5-Fluorotryptophan Spectroscopy Study[†]

Erwin P. P. Vos,[‡] Marcel Bokhove,[‡] Ben H. Hesp,[§] and Jaap Broos*[,‡]

[‡]*Department of Biophysical Chemistry, Groningen Biomolecular Science and Biotechnology Institute, and* [§]*Zernike Institute for Advanced Materials, University of Groningen, Nijenborgh 4, 9747 AG Groningen, The Netherlands*

Received November 7, 2008; Revised Manuscript Received April 28, 2009

ABSTRACT: In this work, four single tryptophan (Trp) mutants of the dimeric mannitol transporter of *Escherichia coli*, EII^{mtl}, are characterized using Trp and 5-fluoroTrp (5-FTrp) fluorescence spectroscopy. The four positions, 97, 114, 126, and 133, are located in a region shown by recent studies to be involved in the mannitol translocation process. To spectroscopically distinguish between the Trp positions in each subunit of dimeric EII^{mtl}, 5-FTrp was biosynthetically incorporated because of its much simpler photophysics compared to those of Trp. The steady-state and time-resolved fluorescence methodologies used point out that all four positions are in structured environments, both in the absence and in the presence of a saturating concentration of mannitol. The fluorescence decay of all 5-FTrp-containing mutants was highly homogeneous, suggesting similar microenvironments for both probes per dimer. However, Stern−Volmer quenching experiments using potassium iodide indicate different solvent accessibilities for the two probes at positions 97 and 133. A 5 Å two-dimensional (2D) projection map of the membrane-embedded IIC^{mtl} dimer showing 2-fold symmetry is available. The results of this work are in better agreement with a 7 Å projection map from a single 2D crystal on which no symmetry was imposed.

Downloaded by UNIV OF GRONINGEN on September 17, 2009 | http://pubs.acs.org
Publication Date (Web): April 29, 2009 | doi: 10.1021/bi8020668

The mannitol permease of *Escherichia coli*, EII^{mtl},[1] is responsible for the transport of mannitol across the cytoplasmic membrane and for its concomitant phosphorylation to mannitol 1-phosphate. The protein belongs to the phosphoenolpyruvate (PEP)-dependent phosphotransferase system (PTS), a system consisting of different sugar-specific EII transporters which phosphorylate their sugar during translocation (*1*, *2*). The phosphate group is donated by PEP and transferred via the cytoplasmic proteins EI and HPr to EII. In EII^{mtl}, the phosphate group is donated to His554 in the A domain and subsequently transferred to Cys384 in the B domain, which phosphorylates mannitol bound at the C domain (IIC^{mtl}). The A and B domains (each 14 kDa) and the C domain (36 kDa) are covalently linked. The three-dimensional (3D) structures of the A and B domains have been determined (*3*, *4*). For the membrane-embedded C domain, harboring the sugar translocation pathway, a 5 Å two-dimensional (2D) projection map is available (*5*). The functional oligomeric state of EII^{mtl} is a dimer, and it contains one mannitol binding site (*6*).

Currently, little is known about the structure of IIC domains of the PTS sugar translocators. Topology studies predict six to eight TMHs (*7*−*9*). Recent studies (*8*, *10*) suggest that residues 70−134, presented as a cytoplasmic loop in the IIC^{mtl} topology model of Sugiyama et al. (*7*) (Figure 1), are involved in the mannitol translocation process. Some of these residues are accessible only from the periplasmic side, while others are accessible only from the cytoplasmic side (*8*). Conformational changes upon mannitol binding or upon EII^{mtl} phosphorylation in this region have been reported (*8*, *10*). Moreover, residue position 124 labeled with a Cys can form a disulfide bridge with Cys384 in the B domain (*11*). In two recent topology models, residues 70−134 are presented as forming two short α-helices, protruding into the membrane (*8*), or presented as a transmembrane helix and a periplasmic loop (*9*). IIC^{mtl} is known to be remarkably resistant to trypsin degradation, and therefore, the cytoplasmic loop formed by residues 70−134 is likely structured.

Tryptophan phosphorescence spectroscopy was used to investigate structural details of this "active" region of the IIC^{mtl} domain (*10*). Four single Trp mutants of EII^{mtl} containing a Trp at positions 97, 114, 126, and 133 were analyzed (mutants W97, W114, W126, and W133, respectively). All mutants were created by F to W substitution in the Trp-less protein. One remarkable outcome of this study was that the microenvironment of W97

[†]This work was supported by The Netherlands Foundation for Chemical Research (CW) with financial aid from The Netherlands Organization for the Advancement of Scientific Research (NWO).

*To whom correspondence should be addressed. Phone: +31 50 3634277. Fax: +31 50 3634800. E-mail: j.broos@rug.nl.

[1]Abbreviations: EII^{mtl}, mannitol-specific transporting and phosphorylating enzyme from *E. coli*; 5-FTrp, 5-fluorotryptophan; 5-FNATA, *N*-acetyl-DL-5-fluorotryptophanamide; PTS, phosphoenolpyruvate-dependent group translocation system; TMH, transmembrane helix; mannitol, D-mannitol; PEP, phosphoenolpyruvate; S−V, Stern−Volmer; fwhh, full width at half-height; TCSPC, time-correlated single-photon counting; EII^{mtl}, wild-type EII^{mtl} with tryptophans at positions 30, 42, 109, and 117; Trp-less EII^{mtl}, EII^{mtl} in which the four native tryptophans are replaced with Phe. W97, W114, W126, and W133 are the single-Trp-containing EII^{mtl} mutants based on Trp-less EII^{mtl}.

 Published on Web 04/29/2009 © 2009 American Chemical Society

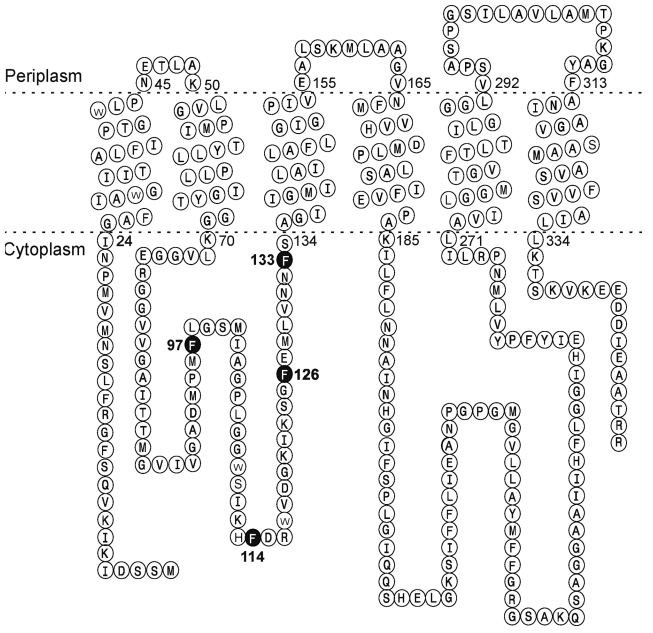

FIGURE 1: Topology of wild-type IIC^{mtl} according to Sugiyama et al. (*7*). The four positions investigated in this work are highlighted in black. Adapted after some modifications from ref *8*.

is very rigid as reflected in a long phosphorescence lifetime (τ_p) of 600 ms in buffer at ambient temperature. In the presence of mannitol, τ_p was reduced one hundred-fold, suggesting that the microenvironment of W97 becomes partly unfolded. Of the eight conditions studied (four mutants in the absence and presence of mannitol), five conditions yielded a short τ_p. In this paper, the microenvironment of the four Trp residues is characterized in more detail using fluorescence spectroscopy. The local flexibility is probed by fluorescence anisotropy decay measurements, indicating that under all eight conditions studied the Trp residues are at structured microenvironments. This result is discussed along with the phosphorescence study.

Since EII^{mtl} is a dimeric protein, two Trp residues are present per functional unit. The collected Trp phosphorescence parameters do represent both Trp residues in dimeric EII^{mtl}, and drawing conclusions about differences in the microenvironment of each individual Trp residue is not straightforward. This limitation can be overcome to some extent by replacing Trp with 5-fluorotryptophan (5-FTrp). 5-FTrp (*12*) can be efficiently (>95%) biosynthetically incorporated into EII^{mtl} using an *E. coli* Trp auxotroph (*13*). Its fluorescence decay is very homogeneous at most protein residue positions studied so far (*14*). Because of its simple decay kinetics, a change in the fluorescence lifetime (τ) of one of the 5-FTrp residues can be distinguished from the unchanged τ of the 5-FTrp residue in the other subunit of the dimer. Most data presented in this work are from 5-FTrp-containing mutants. Differences between the microenvironment of 5-FTrp were observed for two of the four mutants, indicating that homodimeric EII^{mtl} is structurally asymmetrical. This result is discussed in light of two available two-dimensional (2D) projection maps of the membrane-embedded IIC^{mtl} dimer, one on which 2-fold symmetry was imposed and one not showing this symmetry.

EXPERIMENTAL PROCEDURES

Reagents and Proteins. $C_{10}E_5$ detergent was from Kwant High Vacuum Oil Recycling and Synthesis (Bedum, The Netherlands). Fluorescent impurities were removed as described previously (*15*). KI (Suprapur) was from Merck (Darmstadt, Germany). *N*-Acetyl-DL-5-fluorotryptophanamide (5-FNATA) was synthesized as previously described (*16*).

Construction of the single-Trp-containing mutants is presented elsewhere (*33*). Biosynthetic incorporation of 5-FTrp into EII^{mtl} was performed as described previously (*13*). Purification of the proteins followed a published procedure (*17*), except that the thrombin cleavage step of the His tag was omitted. Mannitol binding and the nonvectorial phosphorylation activity, catalyzed by EII^{mtl}, were measured as described previously (*18*, *19*). No changes in the mannitol binding affinity or nonvectorial phosphorylation activity were observed when Trp was replaced with 5-FTrp.

Fluorescence Spectroscopy. All fluorescence experiments were performed in buffer containing 20 mM Tris-HCl (pH 8.4), 250 mM NaCl, 1 mM reduced glutathione, and 0.25% (v/v) $C_{10}E_5$. Fluorescence spectra of the Trp-containing mutants were recorded on an SLM-Aminco SPF-500 fluorometer at room temperature. Excitation was at 295 nm with excitation and emission bandpasses at 2 and 5 nm, respectively. The emission spectra of 5-FTrp-containing mutants were recorded on a Fluorolog3-22 fluorospectrometer (Jobin Yvon) at 23 °C. Excitation was at 295 nm; bandwidths of 1.25 and 7 nm were employed for excitation and emission, respectively. The Stern−Volmer (S−V) experiments with KI as the quencher were performed using these settings. Fluorescence intensities were calculated via integration of the emission peak. Under each condition, the spectra were recorded two or three times and the variation between the integral values was found to be less than 5%. All spectra were corrected for fluorescence from the buffer and for instrument response.

Fluorescence lifetime (TCSPC) measurements were performed at 20 °C using a frequency-tripled modelocked Ti: Sapphire laser system for excitation (Coherent Inc., VERDI-5W, MIRA-900-F, Pulse Picker 9200, Harmonics Generator 9200), delivering subpicosecond pulses of approximately 5 pJ at a 1.9 MHz repetition rate. The fluorescence was collected at 90° via an f/2 collimating lens, a HNP'B near-UV polarizer (3M), and a 368 nm interference filter with a 17 nm fwhm bandpass (Schott). The emission photons were detected with a microchannel plate photomultiplier (Hamamatsu R1564U-01 or R3809U-50). The start signal was provided by a fast photodiode (Becker & Hickel, APM-400) detecting the second harmonic output of the laser system. The single-photon pulses from the detector were fed into a 1.6 GHz amplifier (Becker & Hickel, HFAC-26) whose output was connected to the STOP input of the TCSPC computer card (Edinburgh Instruments TCC900). The signal was collected by automatically switching the emission polarizer between a parallel and perpendicular orientation, every 50 s. The emission decay was stored in 2048 channels (24 ps per channel). Excitation was at 305 nm, and decays of EII^{mtl} mutants were corrected for buffer. *p*-Terphenyl in ethanol was used as the monoexponential deconvolution reference (τ = 1.06 ns). Data were analyzed with a model of discrete exponentials using the TRFA data processing package, version 1.2, of SSTC (Belarusian State University, Minsk, Belarus).

RESULTS

Steady-State Spectra. In Table 1, the emission maxima (λ^{max}) of W97, W114, W126, and W133 containing either Trp or 5-FTrp are presented. For the Trp-containing proteins, W97

Downloaded by UNIV OF GRONINGEN on September 17, 2009 | http://pubs.acs.org
Publication Date (Web): April 29, 2009 | doi: 10.1021/bi8020668

Downloaded by UNIV OF GRONINGEN on September 17, 2009 | http://pubs.acs.org
Publication Date (Web): April 29, 2009 | doi: 10.1021/bi8020668

shows the most blue-shifted λ^{max} (at 318 nm) and W126 the most red-shifted λ^{max} (at 330 nm). For the 5-FTrp-containing proteins, the same trend is visible except that the spectra are approximately 5 nm red-shifted. 5-FTrp emission spectra are known to be slightly red-shifted compared to Trp emission spectra (*16*).

Effect of Mannitol on the Emission Spectra. Mutants W114, W126, and W133 show, like wild-type EII^{mtl}, a high affinity for mannitol ($K_d \sim 100$ nM) (*10*). For W97, a lower affinity was measured ($K_d \sim 2$ μM) (*10*). The effects of a saturating concentration of mannitol (50 μM) on the emission spectra of the Trp-containing mutants are presented in Table 1. Mannitol binding induces only minor changes (<5%) in the spectra of W114 and W126. The emission intensity of W133 increases 5%. For W97, the effect of mannitol is very strong as the emission intensity drops 46%. A similar trend is evident for the 5-FTrp-containing mutants, although the change in emission is significantly smaller for the W97 mutant (−13%). The broadness (fwhh) of the emission spectra of the W97 and W126 mutants, containing 5-FTrp, increases upon mannitol binding, while a narrowing was observed for W133 containing 5-FTrp (Table 1). A measurable change in λ^{max} upon mannitol binding (2 nm) was observed only for W126 containing 5-FTrp.

Time-Resolved Fluorescence Data of 5-FTrp-Containing Mutants. In Figures 2 and 3, the 5-FTrp decays are presented for W97, W114, W126, and W133, together with reduced residuals (χ_r^2) and the autocorrelation function. The fit parameters are listed in Table 2. For W97 and W114, a single exponential could adequately fit the decays. For W126 and W133, three exponentials were needed for a proper fit; the decays are dominated by $\tau = 5.3$ ns ($\alpha = 0.93$) and $\tau = 4.5$ ns ($\alpha = 0.95$) values, respectively. In the presence of mannitol, the fluorescence of W97 decays essentially with the same τ as in the absence of mannitol. A 19% drop in amplitude (α) is detected, showing that the decrease in steady-state emission upon mannitol binding is due to the formation of dark ground-state complexes. Similarly, a drop in α was also observed for W133 (−10% for $\tau = 4.5$ ns), together with no change in τ.

To investigate the microenvironment of the four 5-Trp positions in more detail, the anisotropy decays were recorded in the absence and presence of mannitol (Figure 4 and Table 3). The decays could be properly fitted using two or three rotational correlation times (ϕ). For the sake of clarity, only the modeled fit functions are presented in Figure 4. All anisotropy decays are dominated by $\phi = \infty$, typical for immobilized 5-FTrp side chains. Because dimeric EII^{mtl}, solubilized by detergent, is a large complex (>200 kDa), depolarization due to protein tumbling cannot be assessed with 5-FTrp.

Solvent Accessibility of the 5-FTrp Positions toward KI. Stern−Volmer (S−V) experiments were performed with the four mutants using KI as the collisional quencher. KI and not acrylamide was used as the quencher because the latter likely partitions into the $C_{10}E_5$ micelle surrounding EII^{mtl}, in this way biasing the quenching data. Moreover, acrylamide can quench the singlet Trp state quite efficiently via a through space mechanism (*20*).

EII^{mtl} is a dimeric protein under the conditions used in this work (*21*). When the two 5-FTrp residues in the dimer exhibit similar solvent accessibilities, a linear S−V plot is expected. When the solvent accessibility is different for the two probes, a S−V plot showing a downward curvature is expected (*22*). 5-FTrp at position 126 shows a high and essentially similar solvent accessibility in the presence and absence of mannitol (Figure 5).

Table 1: Steady-State Fluorescence of Single Trp and 5-FTrp-Containing Mutants of EII^{mtl}

	λ^{max} (nm)	emission intensity (% change) with mannitol	fwhh (nm)	fwhh with mannitol (nm)
W97 Trp	318	−46		
W97 5-FTrp	323	−13	44	46.9
W114 Trp	324	3		
W114 5-FTrp	329	3	48.3	48.7
W126 Trp	330	−4		
W126 5-FTrp	334 (336 with mannitol)	0	54.6	55.5
W133 Trp	321	5		
W133 5-FTrp	325	−8	45.7	44.8

For mutant W97 without mannitol, a very low solvent accessibility for KI was measured. In the presence of mannitol, a fraction of the protein becomes more solvent accessible at position 97. The opposite situation was observed for W133; addition of mannitol decreases the accessibility of 5-FTrp at position 133 for KI. The S−V plots for W133 under both conditions show a downward curvature, indicating different microenvironments of each 133 position in the dimer.

Since the quenching of 5-FTrp for KI has not been reported before, the KI sensitivity of this probe was investigated using the neutral analogue 5-FNATA ($\tau = 4.4$ ns) (*14*), dissolved in the same buffer as the EII^{mtl} mutants. A S−V constant of 20 M^{-1} was observed, corresponding to a collisional quenching constant (k_q) of 4.5×10^9 M^{-1} s^{-1}. KI quenching of NATA under these conditions yielded a k_q of 4.3×10^9 M^{-1} s^{-1}. This shows that fluoro substitution of Trp at the 5 position does not affect its sensitivity for quenching by iodide.

DISCUSSION

In this work, a fluorescence study of four single Trp mutants of EII^{mtl}, all containing a Trp in the first putative cytoplasmic loop of the IIC^{mtl} topology model of Sugiyama et al. (*7*), is presented (Figure 1). Comparison of the fluorescence lifetimes, rotational correlation times, and solvent accessibilities, in the absence and presence of mannitol, shows that this part of the protein undergoes large structural changes upon ligand binding. Most of the experiments have been conducted with mutants containing 5-FTrp, biosynthetically incorporated using an *E. coli* Trp auxotroph. In an earlier report, the same positions have been studied using Trp phosphorescence spectroscopy (*10*). Both techniques yield complementary information; in fluorescence, dynamic features on the nanosecond time scale are probed while Trp phosphorescence is remarkably sensitive to the local fluidity and can report on conformational changes in the microsecond to second time domain. A new feature introduced here is the ability to distinguish between the microenvironments of the two Trp positions in each subunit in dimeric EII^{mtl}. For this, we took advantage of the simple fluorescence decay kinetics of 5-FTrp and combined time-resolved data with iodide quenching results.

Comparison of Trp and 5-FTrp as Intrinsic Protein Probes. A difference between Trp and 5-FTrp, relevant for protein fluorescence studies, is the 0.3 eV increase in ionization potential upon 5-fluoro substitution (*16*). The higher ionization potential efficiently suppresses electron transfer from the excited state to nearby amide groups acting as electron acceptors. This photoinduced electron transfer process is the dominant

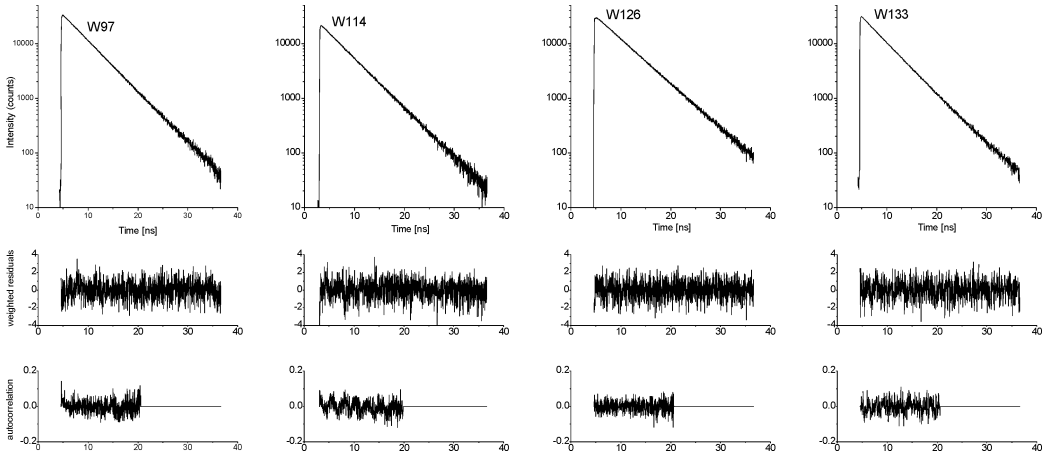

FIGURE 2: Fluorescence decays of single 5-FTrp-containing EII^{mtl} mutants. Experimental fluorescence decays (top panels) of mutants W97, W114, W126, and W133 (from left to right), along with the reduced residuals (middle panels) and the autocorrelation functions of the residuals (bottom panels).

Downloaded by UNIV OF GRONINGEN on September 17, 2009 | http://pubs.acs.org
Publication Date (Web): April 29, 2009 | doi: 10.1021/bi8020668

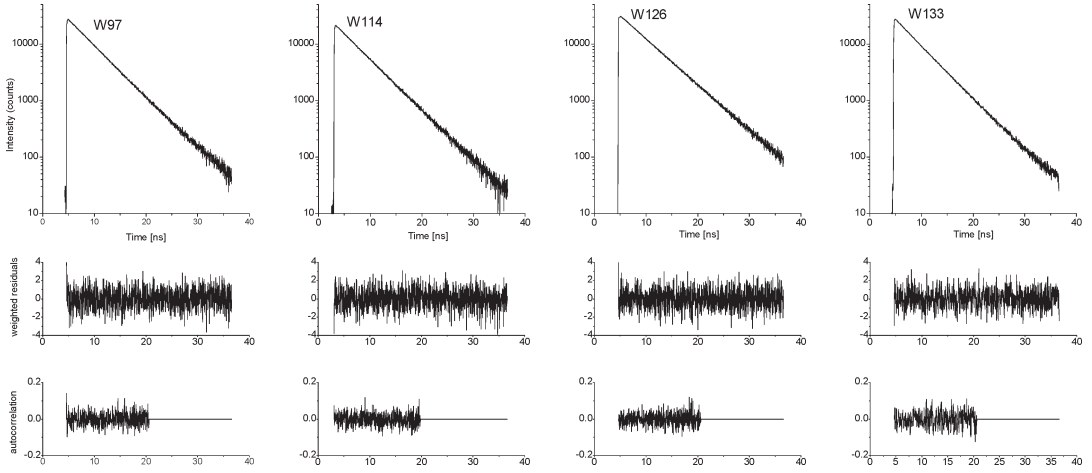

FIGURE 3: Fluorescence decays of single 5-FTrp-containing EII^{mtl} mutants in the presence of 50 μM mannitol. Experimental fluorescence decays (top panels) of mutants W97, W114, W126, and W133 (from left to right), along with the reduced residuals (middle panels) and the autocorrelation functions of the residuals (bottom panels).

Table 2: Time-Resolved Fluorescence Intensity Decay Parameters of Single 5-FTrp-Containing Mutants of EII^{mtl} in the Absence and Presence of Mannitol[a]

	τ_1 (ns)	τ_2 (ns)	τ_3 (ns)	α_1	α_2	α_3	χ_r^2
W97	4.6			1.0			1.01
with mannitol	4.6	8.6		0.98	0.02		1.11
W114	4.7			1.0			1.07
with mannitol	1.6	4.7		0.02	0.98		1.03
W126	0.01	2.2	5.3	0.01	0.06	0.93	1.01
with mannitol	3.0	5.4		0.01	0.99		1.07
W133	0.9	4.5	8.3	0.03	0.95	0.02	1.01
with mannitol	1.2	4.6	13.0	0.04	0.95	0.01	0.95

[a] The total intensity was assumed as $I(t) = \sum_i \alpha_i \exp(-t/\tau_i)$, where $\sum_i \alpha_i = 1$.

nonradiative depopulation process of the Trp singlet state (*23*). The large variation in quantum yield (Q) observed for Trp in different proteins could be related to the tuning of this process by the protein matrix (*24*). 5-Fluoro substitution in Trp increases the Q and τ by ~50% (*14*). It also reduces the fluorescence decay heterogeneity found for Trp embedded in proteins since each rotamer is either not or only minimally quenched by amide groups, an observation that explains the monoexponential decay often observed for 5-FTrp in proteins (*16*, *25*). Compared to that of Trp, less variation in Q is expected for 5-FTrp-containing proteins undergoing a conformational change since a new established rotamer population likely yields a similar Q. The data presented in Table 1 show that the variation in Q, induced by mannitol binding, is equal or smaller for the 5-FTrp-containing proteins than for the Trp-containing proteins.

Isolation of a new batch of protein can result in a Trp rotamer distribution which differs from a previous batch since the rotamer distribution, "frozen" by the protein matrix, can be dependent on experimental conditions used during isolation. We noticed that the reproducibility of the lifetime of 5-FTrp-containing proteins was very high; typically, a variation of < 0.2 ns was found between different protein batches. The low dependence on the lifetime for the rotamer distribution might be the reason for this.

Below the spectral properties of each mutant are discussed followed by a discussion of what information this work provides about the presence of (a)symmetry in the EII^{mtl} dimer.

W97. The λ^{max} of Trp in W97 is 318 nm, typical for a Trp in either a hydrophobic (*26*) or a rigid environment, where the stabilization of the large excited-state dipole moment of Trp is limited (*27*). The position of the 0−0 vibrational band in the phosphorescence spectrum of W97 was typical for a polar site. On the basis of all the phosphorescence data recorded, it could be

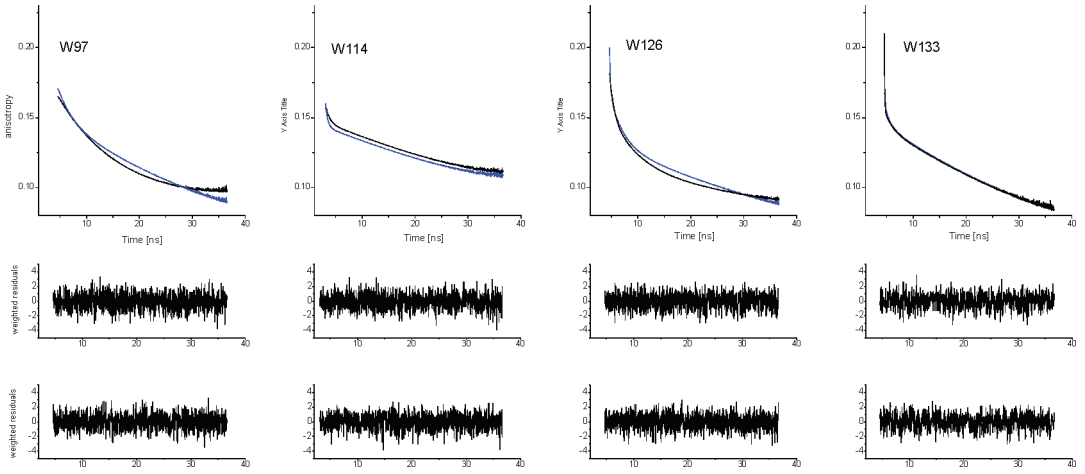

FIGURE 4: Anisotropy decays of single 5-FTrp-containing EII^{mtl} mutants in the absence and presence of 50 μM mannitol. Fitted anisotropy decay functions (top panels) of mutants W97, W114, W126, and W133 (from left to right) without (black) and with 50 μM mannitol (blue), along with the reduced residuals without (middle panels) and with (bottom panels) 50 μM mannitol.

Downloaded by UNIV OF GRONINGEN on September 17, 2009 | http://pubs.acs.org
Publication Date (Web): April 29, 2009 | doi: 10.1021/bi8020668

Table 3: Time-Resolved Fluorescence Anisotropy Decay Parameters of Single 5-FTrp-Containing Mutants of EII^{mtl} in the Absence and Presence of Mannitol[a]

	ϕ_1 (ns)	ϕ_2 (ns)	ϕ_3 (ns)	β_1	β_2	β_3	χ_r^2
W97	11.5	∞		0.08	0.09		1.03
with mannitol	2.91	∞		0.02	0.15		1.08
W114	0.75	∞		0.01	0.15		1.06
with mannitol	0.4	∞		0.02	0.14		1.03
W126	0.8	5.6	∞	0.03	0.04	0.11	0.99
with mannitol	0.17	2.6	∞	0.04	0.04	0.13	1.03
W133	0.03	1.5	∞	0.03	0.01	0.14	1.01
with mannitol	0.2	1.5	∞	0.01	0.01	0.14	0.97

[a] The anisotropy decay was assumed as $r(t) = \sum_i \beta_i \exp(-t/\phi_i)$, $r(0) = \sum_i \beta_i$, $\phi = \infty$ corresponds with $\phi > 10\tau$.

concluded that Trp at position 97 is embedded at a very rigid site (*10*). The low accessibility of W97, containing 5-FTrp, toward KI quenching (Figure 5A) and the slow anisotropy decay (Figure 4) confirm this.

Mannitol binding induces large changes in the microenvironment of position 97. The Trp emission intensity drops 46%, a result that might reflect almost complete quenching of one Trp per functional W97 dimer. With 5-FTrp, the intensity drops by only 13% upon mannitol binding, and the analysis of the fluorescence shows that this drop is due to formation of dark ground-state complexes; the τ remains the same while the amplitude decreases. The increase in the fwhh of the emission spectrum upon mannitol binding and a S−V plot with a downward curvature are in line with an increase in the heterogeneity of the microenvironment of 5-FTrp in the W97 dimer. In the phosphorescence experiments, mannitol binding induced a 100-fold drop in average τ_p for both Trp residues per dimer to 6 ms, a τ_p value similar to that found for free indole in solution (*28*). This result was interpreted as extensive unfolding of the local secondary structure at both 97 positions in the dimer upon mannitol binding. The fluorescence data show that although the structural heterogeneity increases, both 97 positions do not become solvent exposed, since no efficient quenching by KI, a red shift in λ^{max}, or a fast ϕ is observed. Both Trp residues are still at buried positions, one more occluded than the other. Thus, EII^{mtl} is structurally asymmetric at this part of dimeric IIC^{mtl}.

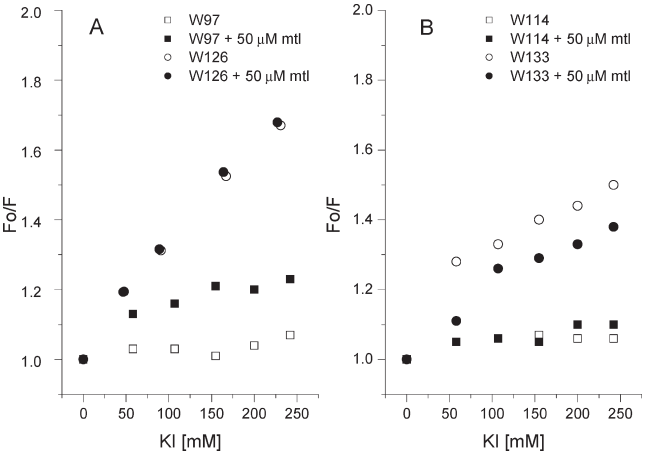

FIGURE 5: Stern−Volmer plots for quenching of single 5-FTrp-containing mutants of EII^{mtl} in the absence and presence of 50 μM mannitol with KI. (A) W97 with or without 50 μM mannitol and W126 with or without 50 μM mannitol. (B) W114 with or without 50 μM mannitol and W133 with or without 50 μM mannitol. F_0 and F are the integrated emission intensities in the absence and presence of KI, respectively.

W114. The anisotropy decay data show that position 114 is almost completely immobilized. In the phosphorescence study (*10*), a very short τ_p of 1.4 ms was observed, a value typical for exposed Trp or Trp quenched by a nearby group like cysteine, cystine, protonated histidine, tyrosine, or phenylalanine (*29*). With the available fluorescence data, we can now attribute the short τ_p to the presence of such a group near position 114. Position 114 is essentially inaccessible for KI quenching in the presence and absence of mannitol. Therefore, the S−V data do not show if structural differences are present between the two 114 positions in the dimer. The homogeneous fluorescence decay of W114 suggests that structural differences are small if present.

W126. The λ^{max} values of Trp and 5-FTrp in W126 are the most red-shifted of the values of the four mutants presented in this work. The τ of 5-FTrp (5.3 ns, $\alpha = 0.93$) is the longest τ reported so far for a 5-FTrp-containing protein showing a homogeneous decay. The anisotropy decay is dominated by $\phi = \infty$, reflecting low-frequency motions at this position. Mannitol binding increases the side chain mobility. W126 is the

Downloaded by UNIV OF GRONINGEN on September 17, 2009 | http://pubs.acs.org
Publication Date (Web): April 29, 2009 | doi: 10.1021/bi8020668

only mutant presented in this study for which an essentially linear S−V relation was observed, and mannitol binding had no measurable impact on solvent accessibility. Apparently, the solvent accessibility of both 5-FTrp positions in the dimer is similar. A k_q of 6.2×10^8 M^{-1} s^{-1} could be calculated, a value 7 times lower that the k_q of 5-FNATA under these conditions (see above).

W133. The λ^{max} of Trp in W133 is at a blue position; binding of mannitol induces a 5% increase in intensity for the Trp-containing protein, while a decrease of 8% is observed with 5-FTrp at position 133. Analysis of the 5-FTrp fluorescence decay showed that this decrease can be attributed to the formation of dark ground-state complexes (Table 2).

The characterization of W133 using phosphorescence spectroscopy revealed a remarkable structuring of the triplet emission spectrum upon mannitol binding, as well as a 4-fold increase in the average τ_p (*10*). This mannitol binding-induced structuring is also reflected in the S−V plot. It makes position W133 less sensitive to KI quenching (Figure 5) and induces a sharpening of the emission spectrum (Table 1). In the anisotropy decay, a fast component (ϕ = 0.03 ns), typical of a freely rotating 5-FTrp side chain, increases to 0.2 ns upon mannitol binding, an observation in line with the phosphorescence and S−V data. The S−V data also reveal different solvent accessibilities for both W133 positions in dimeric EII^{mtl}. Like at position 97, EII^{mtl} is structurally different at both 133 positions in the dimer.

Asymmetry in Dimeric EII^{mtl}. S−V plots showing downward curvature as obtained for W97 and W133 suggest that the two 5-FTrp residues in the dimer have different microenvironments. However, the fluorescence decay kinetics of the four mutants in the absence and presence of mannitol are very homogeneous, indicating that both 5-FTrp residues in each dimer exhibit the same lifetime. Earlier, we reported a linear correlation between the τ of 5-FTrp-containing EII^{mtl} mutants and λ^{max}, and a slope of 0.06 ns/nm was found (*16*). A similar relationship with a positive slope between τ and the λ^{max} of indole derivatives solubilized in aqueous and organic solvents has been reported (*30*). Thus, only a change in microenvironment resulting in a significant shift in λ^{max} of 5-FTrp is expected to have a measurable effect on τ. The solvent dependence of the 5-FTrp λ^{max} is similar to that for Trp (*16*), and the λ^{max} of Trp in proteins is known to vary from 304 nm in a mutant of transhydrogenase from *Rhodospirillum rubrum* (*31*) to 350 nm when at a water-exposed position.

The presence of two different lifetimes in each mutant was analyzed by fitting the fluorescence decay with an extra exponential while splitting the amplitudes of the main lifetime contribution in equal halves and fixing these values during the fitting. In this way, the data can be properly fitted (Table 4), although the fit statistics are not quite as good as the fits presented in Table 2. The obtained fit results show that the two τ values differ by ≤0.2 ns from the τ (Table 2) found for that protein. Therefore, the current time-resolved data sets show no evidence for the presence of large differences in the decay kinetics of the two 5-FTrp residues in each dimer.

New Insights into the Structure and Mechanism of EII^{mtl}. In the phosphorescence study of the four mutants, short τ_p values, typical for free indole, were found under five of the eight conditions studied (four mutants in the absence and presence of mannitol). The τ_p value of a single Trp-containing protein in buffer at ambient temperature is the most informative phosphorescence parameter for the local structure as a good empirical relation between τ_p and local viscosity has been presented (*32*). However, this relationship breaks down if the Trp is close to a nearby quenching group like cysteine, cystine, protonated histidine, tyrosine, or phenylalanine (*29*). This work clearly demonstrates that the four studied Trp positions are at structured positions as for each mutant a large contribution of immobilized 5-FTrp is present in the anisotropy decay (ϕ = ∞), both in the absence and in the presence of mannitol. The S−V data are also in line with the Trp residues at structured positions as the solvent accessibility for iodide ranged from a limited accessibility (W126) to inaccessible in the case of W114. The solvent accessibility of these four Trp positions has not been reported previously. Interestingly, the S−V data together with the fluorescence decay kinetics inform about the presence and extent of (a)symmetry in dimeric EII^{mtl}. As for each mutant a homogeneous decay was recorded, one can conclude that structural differences between the two Trp microenvironments in the dimer are of limited order. S−V data for W97 and W133 disclose differences in structure between the subunits.

Structural differences between equal residue positions in dimeric EII^{mtl} were not expected. In the published 5 Å projection map of dimeric EII^{mtl}, two subunits with the same electron density distribution are visible, because 2-fold symmetry was imposed. Electron microscopy data from different 2D crystals was used for this projection map (Figure 6B). The authors also presented a 7 Å projection map obtained from one 2D crystal on

Table 4: Time-Resolved Fluorescence Intensity Decay Parameters of Single 5-FTrp-Containing Mutants of EII^{mtl} in the Absence and Presence of Mannitol, Obtained When Fitting the Data with Two Equal and Fixed Values of α[a]

	τ_1 (ns)	τ_2 (ns)	τ_3 (ns)	τ_4 (ns)	α_1	α_2	α_3	α_4	χ_r^2
W97	4.4	4.5			0.50	0.50			1.00
with mannitol	4.5	4.7	8.6		0.49	0.49	0.02		1.13
W114	4.7	4.5			0.50	0.50			1.08
with mannitol	4.7	4.7	1.6		0.49	0.49	0.02		1.04
W126	5.2	5.5	2.4	0.01	0.47	0.47	0.06	0.01	1.01
with mannitol	5.4	5.4	3.0		0.49	0.49	0.02		1.11
W133	4.4	4.7	1.0	8.5	0.47	0.47	0.03	0.03	1.08
with mannitol	4.6	4.7	1.6	23.0	0.47	0.47	0.05	0.01	1.02

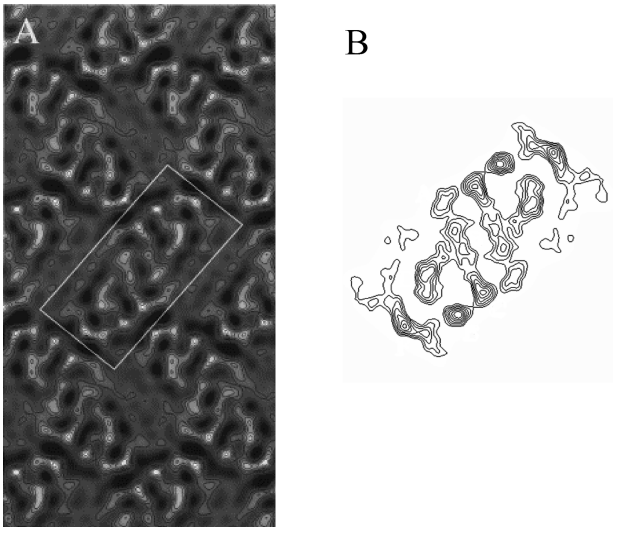

FIGURE 6: 2D projection maps of IIC^{mtl} (*5*): (A) 7 Å projection map from a single IIC^{mtl} 2D crystal on which no symmetry was imposed (one IIC^{mtl} dimer enclosed in a white box) and (B) 5 Å projection map, calculated by using data from different IIC^{mtl} crystals and imposing 2-fold symmetry. These panels were adapted with minor modifications from ref *5*.

which no 2-fold symmetry was imposed (Figure 6A). Here small differences in electron density are visible between the two subunits at many positions. The spectral data presented in this paper support the view that these differences represent the structure of dimeric IIC^{mtl} in solution. Whether dimeric IIC^{mtl} shows 2-fold symmetry is significant for the mechanism of this transporter. If symmetry is present, the position of the single mannitol binding site present per dimer is expected at the dimer interface and centered at the 2-fold symmetry axis. In this model, pairs of residues from each subunit form the mannitol binding site and the mannitol translocation pathway. Monomeric IIC^{mtl} does not exhibit affinity for mannitol, and the oligomerization to dimers thus induces conformational changes to bind mannitol with high affinity. When IIC^{mtl} forms an asymmetric dimer this way, mannitol binding and translocation can in principle take place at any position at the dimer interface or within one subunit. The results presented in this paper will stimulate more work to establish the structural organization of dimeric EII^{mtl}. Given the difficulty in crystallizing membrane proteins, extending the approach used in this work with many more mutants is an attractive alternative for achieving this goal.

Downloaded by UNIV OF GRONINGEN on September 17, 2009 | http://pubs.acs.org
Publication Date (Web): April 29, 2009 | doi: 10.1021/bi8020668

ACKNOWLEDGMENT

We thank Foppe de Haan for writing software enabling switching of the orientation of the polarizers and processing the raw time-resolved fluorescence data in a format that can be recognized by the time-resolved analysis software.

REFERENCES

1. Lengeler, J. W., Jahreis, K., and Wehmeier, U. F. (1994) Enzymes II of the phospho enol pyruvate-dependent phosphotransferase systems: Their structure and function in carbohydrate transport. *Biochim. Biophys. Acta 1188*, 1–28.
2. Robillard, G. T., and Broos, J. (1999) Structure/function studies on the bacterial carbohydrate transporters, enzymes II, of the phosphoenolpyruvate-dependent phosphotransferase system. *Biochim. Biophys. Acta 1422*, 73–104.
3. van Montfort, R. L. M., Pijning, T., Kalk, K. H., Hangyi, I., Kouwijzer, M. L. C. E., Robillard, G. T., and Dijkstra, B. W. (1998) The structure of the *Escherichia coli* phosphotransferase IIA (mannitol) reveals a novel fold with two conformations of the active site. *Structure 6*, 377–388.
4. Legler, P. M., Cai, M. L., Peterkofsky, A., and Clore, G. M. (2004) Three-dimensional solution structure of the cytoplasmic B domain of the mannitol transporter IIMannitol of the *Escherichia coli* phosphotransferase system. *J. Biol. Chem. 279*, 39115–39121.
5. Koning, R. I., Keegstra, W., Oostergetel, G. T., Schuurman Wolters, G., Robillard, G. T., and Brisson, A. (1999) The 5 Å projection structure of the transmembrane domain of the mannitol transporter enzyme II. *J. Mol. Biol. 287*, 845–851.
6. Veldhuis, G., Broos, J., Poolman, B., and Scheek, R. M. (2005) Stoichiometry and substrate affinity of the mannitol transporter, Enzymell(mtl), from *Escherichia coli*. *Biophys. J. 89*, 201–210.
7. Sugiyama, J. E., Mahmoodian, S., and Jacobson, G. R. (1991) Membrane topology analysis of *Escherichia coli* mannitol permease by using a nested-deletion method to create mtlA-phoA fusions. *Proc. Natl. Acad. Sci. U.S.A. 88*, 9603–9607.
8. Vervoort, E. B., Bultema, J. B., Schuurman-Wolters, G. K., Geertsma, E. R., Broos, J., and Poolman, B. (2005) The first cytoplasmic loop of the mannitol permease from *Escherichia coli* is accessible for sulfhydryl reagents from the periplasmic side of the membrane. *J. Mol. Biol. 346*, 733–743.
9. Nguyen, T. X., Yen, M. R., Barabote, R. D., and Saier, M. H. (2006) Topological predictions for integral membrane permeases of the phosphoenolpyruvate: Sugar phosphotransferase system. *J. Mol. Microbiol. Biotechnol. 11*, 345–360.
10. Veldhuis, G., Gabellieri, E., Vos, E. P. P., Poolman, B., Strambini, G. B., and Broos, J. (2005) Substrate-induced conformational changes in the membrane-embedded IICmtl-domain of the mannitol permease from *Escherichia coli*, EnzymeII(mtl), probed by tryptophan phosphorescence spectroscopy. *J. Biol. Chem. 280*, 35148–35156.
11. van Montfort, B. A., Schuurman-Wolters, G. K., Duurkens, R. H., Mensen, R., Poolman, B., and Robillard, G. T. (2001) Cysteine cross-linking defines part of the dimer and B/C domain interface of the *Escherichia coli* mannitol permease. *J. Biol. Chem. 276*, 12756–12763.
12. Ross, J. B. A., Rusinova, E., Luck, L. A., and Rousslang, K. W. (2000) Spectral enhancement of proteins by in vivo incorporation of tryptophan analogues. In *Protein Fluorescence*, pp 17−42, Kluwer Academic/Plenum Publishers, New York.
13. Broos, J., Gabellieri, E., Biemans-Oldehinkel, E., and Strambini, G. B. (2003) Efficient biosynthetic incorporation of tryptophan and indole analogs in an integral membrane protein. *Protein Sci. 12*, 1991–2000.
14. Broos, J., Maddalena, F., and Hesp, B. H. (2004) In vivo synthesized proteins with monoexponential fluorescence decay kinetics. *J. Am. Chem. Soc. 126*, 22–23.
15. Swaving Dijkstra, D., Broos, J., and Robillard, G. T. (1996) Membrane proteins and impure detergents: Procedures to purify membrane proteins to a degree suitable for tryptophan fluorescence spectroscopy. *Anal. Biochem. 240*, 142–147.
16. Liu, T. Q., Callis, P. R., Hesp, B. H., de Groot, M., Buma, W. J., and Broos, J. (2005) Ionization potentials of fluoroindoles and the origin of nonexponential tryptophan fluorescence decay in proteins. *J. Am. Chem. Soc. 127*, 4104–4113.
17. Broos, J., Strambini, G. B., Gonnelli, M., Vos, E. P. P., Koolhof, M., and Robillard, G. T. (2000) Sensitive monitoring of the dynamics of a membrane-bound transport protein by tryptophan phosphorescence spectroscopy. *Biochemistry 39*, 10877–10883.
18. Veldhuis, G., Vos, E. P. P., Broos, J., Poolman, B., and Scheek, R. M. (2004) Evaluation of the flow-dialysis technique for analysis of protein-ligand interactions: An experimental and a Monte Carlo study. *Biophys. J. 86*, 1959–1968.
19. Robillard, G. T., and Blaauw, M. (1987) Enzyme II of the *Escherichia coli* phosphoenolpyruvate-dependent phosphotransferase system: Protein-protein and protein-phospholipid interactions. *Biochemistry 26*, 5796–5803.
20. Cioni, P., and Strambini, G. B. (1998) Acrylamide quenching of protein phosphorescence as a monitor of structural fluctuations in the globular fold. *J. Am. Chem. Soc. 120*, 11749–11757.
21. Broos, J., ten Hoeve Duurkens, R. H., and Robillard, G. T. (1998) A mechanism to alter reversibly the oligomeric state of a membrane-bound protein demonstrated with *Escherichia coli* EII^{mtl} in solution. *J. Biol. Chem. 273*, 3865–3870.
22. Lakowicz, J. R. (2006) *Principles of Fluorescence Spectroscopy*, Springer, New York.
23. Chen, Y., and Barkley, M. D. (1998) Toward understanding tryptophan fluorescence in proteins. *Biochemistry 37*, 9976–9982.
24. Callis, P. R., and Vivian, J. T. (2003) Understanding the variable fluorescence quantum yield of tryptophan in proteins using QM-MM simulations. Quenching by charge transfer to the peptide backbone. *Chem. Phys. Lett. 369*, 409–414.
25. Winkler, G. R., Harkins, S. B., Lee, J. C., and Gray, H. B. (2006) α-Synuclein structures probed by 5-fluorotryptophan fluorescence and F-19 NMR spectroscopy. *J. Phys. Chem. B 110*, 7058–7061.
26. Eftink, M. R. (1991) Fluorescence techniques for studying protein-structure. *Methods Biochem. Anal. 35*, 127–205.
27. Galley, W. C. (1976) Heterogeneity in protein emission spectra. In *Biochemical Fluorescence: Concepts* (Chen, R. F., and Edelhoch, H., Eds.) pp 409−439, Dekker, New York.
28. Strambini, G. B., Kerwin, B. A., Mason, B. D., and Gonnelli, M. (2004) The triplet-state lifetime of indole derivatives in aqueous solution. *Photochem. Photobiol. 80*, 462–470.
29. Gonnelli, M., and Strambini, G. B. (2005) Intramolecular quenching of tryptophan phosphorescence in short peptides and proteins. *Photochem. Photobiol. 81*, 614–622.
30. Meech, S. R., Phillips, D., and Lee, A. G. (1983) On the nature of the fluorescent state of methylated indole-derivatives. *Chem. Phys. 80*, 317–328.
31. Broos, J., Tveen-Jensen, K., de Waal, E., Hesp, B. H., Jackson, J. B., Canters, G. W., and Callis, P. R. (2007) The emitting state of tryptophan in proteins with highly blue-shifted fluorescence. *Angew. Chem., Int. Ed. 46*, 5137–5139.
32. Gonnelli, M., and Strambini, G. B. (1995) Phosphorescence lifetime of tryptophan in proteins. *Biochemistry 34*, 13847–13857.
33. Vos, E. P., Ter Horst, R., Poolman, B., and Broos, J. (2009) Domain complementation studies reveal residues critical for the activity of the mannitol permease from *Escherichia coli*. *Biochim. Biophys. Acta 1788*, 581–586.